Lyotropic Rod−Coil Poly(amide-*block*-aramid) Alternating Block Copolymers: Phase Behavior and Structure

Christiaan de Ruijter, Wolter F. Jager, Liangbin Li,† and Stephen J. Picken*

Nano Structured Materials, Faculty of Applied Sciences, Delft University of Technology, Julianalaan 136, 2628 BL, Delft, The Netherlands

Received October 14, 2005; Revised Manuscript Received April 10, 2006

ABSTRACT: We present results of the phase behavior in sulfuric acid and a structural investigation in the solid state by DSC and SAXS of a series of rod−coil multiblock copolymers comprised of alternating poly(*p*-phenylene terephthalamide) (PPTA) and polyamide 6,6 (PA 6,6) blocks. These polymers were synthesized via a low-temperature polycondensation reaction as described in the first paper of this series. Concentrated solutions of the copolymers in sulfuric acid show a liquid crystalline phase if the mole fraction of PPTA exceeds 0.5. The critical concentration for the transition from the isotropic to the liquid crystalline state increases with increasing amount of flexible PA 6,6 segments. Comparison of the phase behavior of the copolymer with that of PPTA provides strong evidence that the coils in the copolymer are significantly stretched in the nematic solutions. Without solvent, DSC experiments show that the crystallization of the PA 6,6 is to a large extent suppressed by the presence of PPTA, but the degree of crystallization increases upon annealing. SAXS experiments revealed that, although some block copolymers show a peak in the SAXS data, there is no evidence for long-range lamellar order in any block copolymer due to the absence of higher order peaks.

Introduction

In a previous publication we reported the synthesis of a series of rod−coil poly(amide-*b*-aramid) alternating multiblock copolymers using a low-temperature polycondensation method.[1] From a combination of viscosimetry, TGA, and ^{1}H NMR and via an extraction procedure it was shown that a block copolymer was obtained. In the present article we report on the phase behavior of the block copolymers both in solution and in the solid state as a function of polymer composition. It is commonly accepted that block copolymers comprised of alternating rigid and flexible segments are potentially able to form liquid crystalline (LC) phases; however, only a limited number of reports on liquid crystalline block copolyamides with segments of different rigidity have appeared in the literature. Most reports on rod−coil block copolyamides deal with synthesis of the materials for the purpose of preparing molecular composites. So far, two articles dealing with the lyotropic behavior of wholly aromatic block copolamides have been published. Krigbaum et al.[2] reported on the phase behavior of multiblock copolymers composed of rigid poly(*p*-benzamide) (PBA) blocks and the flexible blocks composed of polyterephthalamide of *p*-aminobenzhydrazide (PABH-T) or poly(*m*-phenylene isophthalamide) (MDP-I) that were dissolved in *N*,*N*-dimethylacetamide (DMAc) containing 3% LiCl. Later Cavalleri et al.[3,4] extended the work of Krigbaum and reported on the phase behavior of diblock copolymers of PBA with either MDP-I[3] or poly(*m*-benzamide)[4] as the flexible block in the same solvent system. Cavalleri synthesized tailored diblock copolymers in order to more accurately compare the phase behavior with the theoretical models of Matheson−Flory[5] and Vasilenko.[6] The authors observed that a block copolymer bearing a longer flexible block than allowed by the Matheson−Flory model was still able to form a LC phase. The authors attributed this to partial ordering of the flexible component by the self-consistent orientational field of the rigid component. In the Matheson−Flory model[5] chain stretching is not taken into account, and the flexible chains only act as a diluent for the mesophase. The authors concluded that it would be better to compare the phase behavior with the Vasilenko model because this model does account for conformational changes of the flexible component by the orientational field of the mesophase. In addition, the authors observed an increased stability of the mesophase when a semiflexibe chain was coupled to a rigid homopolymer, which means that the concentration range where the mesophase was present was considerably increased. This was concluded from the observations that although the critical concentration for mesophase formation was slightly increased, the biphasic gap was strongly reduced and also the solubility of the copolymer was strongly enhanced compared to the rigid homopolymer. To relate the phase behavior of the block copolymers to the model, the authors constructed phase diagrams as a function of concentration and composition at a fixed (ambient) temperature since both the Matheson−Flory and Vasilenko theories originate from athermal lattice models.

In the present paper we report on the phase behavior as a function of composition, concentration, and temperature, which means that evaluation of the obtained results with athermal theories is not applicable. However, Yurasova and Semenov[7] as well as Wang and Warner[8] recently developed more sophisticated models based on a mean-field approach of the Maier−Saupe[9,10] type that describes temperature-dependent phase behavior of block copolymers with rigid and flexible segments. In this paper we will compare our results to a modified Maier−Saupe mean-field theory adapted by Picken[11] in order to estimate the effective persistence length of the block copolymers in sulfuric acid.

The second part of this paper concerns the structural investigation of the copolymers in the solid state. Structural investigation of LC rod−coil block copolyamides in the solid state is not common although it is commonly accepted that,

† Current address: Unilever Res. & Dev. Vlaardingen, Olivier van Noortlaan 120, Vlaardingen, NL-3133 AT Netherlands.

* Corresponding author: e-mail S.J.Picken@tnw.tudelft.nl; Tel +31 15 2786946; Fax +31 15 2787415.

10.1021/ma052230+ CCC: $33.50
Published on Web 05/23/2006

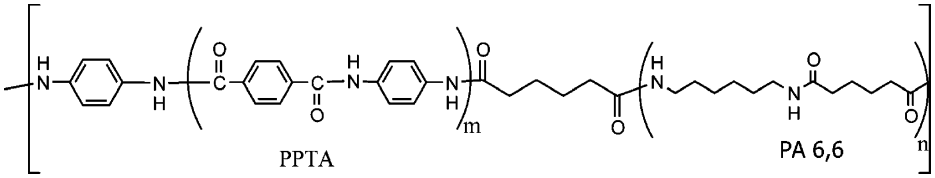

Figure 1. Chemical structure of a PPTA-*b*-PA-6,6 block copolymer.

Table 1. Inherent Viscosities and Composition of the Studied Copolymers

polymer	η_{inh} (dL g^{-1})	M_w[a]	amount of flexible (PA 6,6) block (mol %)	no. of repeat units[b] of PPTA m[c]	no. of repeat units[b] of PA n[c]
P10-4	1.87	11 000	29	10	4
P10-10	1.71	11 600	50	10	10
P4-4	2.06	17 200	50	4	4
P4-10	0.75	7 200	71	4	10

[a] Polystyrene equivalent molar masses as obtained by using SEC.[1] [b] Theoretical degree of polymerization depends on stoichiometry. [c] m and n refer to Figure 1.

due to incompatibility of the components, a block copolymer material will tend to phase separate and may possibly show long-range order if the polydispersity of the blocks is narrow. A rod−coil block copolymer will display even higher incompatibility because of the strong structural difference between the blocks that results in an increased tendency toward phase separation.[12] To our knowledge the only structural study of monodisperse rod−coil block multiblock copolymers has been done by Lee et al.[13] The authors synthesized a series of rod−coil copolymers of which the rigid rod segments were made up of three biphenyls connected through methylene ether linkages, and the flexible segments were made of poly(propylene oxide) with a degree of polymerization of 13. By using SAXS, the authors observed that the diblock copolymer displayed a lamellar structure and the multiblock copolymers with a number of repeating units of 3 and more displayed a hexagonal columnar phase. The authors also observed a rapid decrease of the long period of the observed structure with increasing number of repeating units.

In the present study the polydispersity index of the block copolyamides is rather high, and therefore the formation of well-defined long-range ordered structures is not anticipated. Small-angle X-ray scattering (SAXS) measurements and differential scanning calorimetry (DSC) have been performed in order to get better insight into the extent of phase separation in the copolymers and the melting and crystallization behavior of the PA6,6 blocks, respectively.

Experimental Section

Synthesis. A series of four block copolymers composed of alternating blocks of PPTA (polyphenylene terephthalamide) and PA 6,6 (polyamide 6,6) were synthesized by a two-step low-temperature polycondensation procedure in *N*-methyl-2-pyrrolidinone (NMP) containing about 10 wt % $CaCl_2$, as described in part 1.[1] The chemical structure of a repeat unit of the block copolymer is shown in Figure 1, and Table 1 summarizes some characteristics of the block copolymers.

Measurements. Nematic−isotropic transition (clearing) temperatures were determined as a function of polymer concentration in sulfuric acid by OPM (optical polarization microscopy). A Nikon Eclipse E600 Pol. polarizing microscope equipped with a Mettler-Toledo FP82HT hot-stage was used.

Differential scanning calorimetric (DSC) measurements were performed with a Perkin-Elmer TAC 7/DX DSC. All samples were heated from 25 to 325 °C, next cooled to 25 °C, and heated again to 325 °C. The heating and cooling rates were 10 °C/min.

Small-angle X-ray scattering (SAXS) experiments were performed on finely powdered copolymer samples at the SAXS facility at the FOM Institute for Atomic and Molecular Physics (Amolf) in Amsterdam, The Netherlands. In this setup a rotating anode X-ray generator generates a highly parallel beam of monochromatic Cu Kα radiation. A Linkam CSS450 shear cell was used as a sample stage. A brass sample holder with Kapton windows was used to replace the original glass windows. The SAXS patterns were recorded with a Bruker High-Star area detector. The two-dimensional SAXS patterns were integrated azimuthally and corrected for the background to obtain one-dimensional plots of the intensity as a function of the scattering vector $q = 4\pi \sin \theta/\lambda$, where λ is the X-ray wavelength (0.154 nm) and 2θ the scattering angle.

Results and Discussion

Solution Properties. a. Phase Behavior in Sulfuric Acid. The phase behavior of PPTA−PA 6,6 block copolymers in 100% sulfuric acid as a function of temperature was examined by OPM. Because of the high viscosity of the polymeric samples, phase transitions are not instantaneous. In addition, because we are dealing with polymer solutions, there is a temperature range where the isotropic and nematic phases coexist. The obtained phase diagrams are shown in Figure 2. The upper curve describes the transition from the biphasic (I + LC) to the isotropic (I) phase, and the bottom curve describes the transition of the LC phase to the biphasic region. To construct a phase diagram, five different polymer concentrations were measured at a heating rate of 4 °C/min. Each polymer concentration was measured at least five times. By taking the average of these measurements, reasonably accurate and reproducible values of the transition temperatures were obtained. According to Figure 2, all copolymers show LC behavior when dissolved in sulfuric acid although in sample **P4-10** only very weak birefringence was observed. The observed texture of this sample might indicate a phase-separated structure rather than a LC phase.

To compare the phase behavior of the polymer samples, Figure 3 shows the clearing temperature T_{ni} at which 50% phase transition is observed vs polymer concentration. In this figure the phase behavior of the copolymer samples, a high molecular weight PPTA sample (η_{inh} = 4.2 dL/g, M_w = 32 000) and a low molecular weight PPTA-oligomer with a number of repeat units of m = 4 (η_{inh} = 0.42 dL/g), is shown. From Figure 3 it is clear that the critical concentration for the formation of a LC phase increases with increasing fraction of the flexible fragments in the block copolymer. Another striking observation that results from Figure 3 is that coupling of flexible chains to rodlike oligomers increases the stability of the LC phase, i.e., the LC phase of copolymer **P4-4** shows a greater thermal stability compared to the PPTA oligomer (**P4-0**), whereas the average lengths of the rigid units in the copolymer and the oligomer are the same. Another indication of the increased stability of the LC phase of the block copolymer can be seen when we compare the curve of sample **P4-4** with the curve of pure PPTA. Pure PPTA shows a LC to I transition at ambient temperature at about 8 wt %. If the flexible segments in the copolymer only would act as a diluent, the phase transition for sample **P4-4**

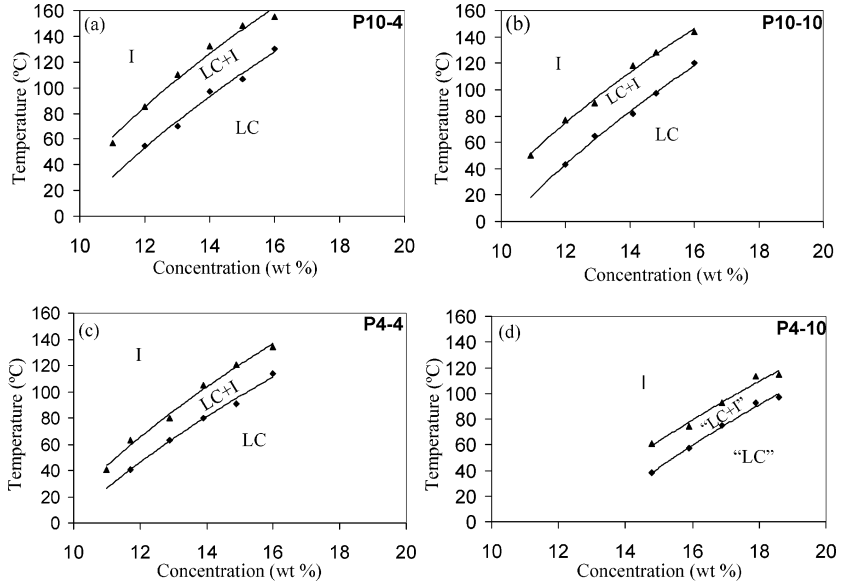

Figure 2. Phase behavior of copolymer samples **P10-4** (a), **P10-10** (b), **P4-4** (c), and **P4-10** (d) in 100% H_2SO_4.

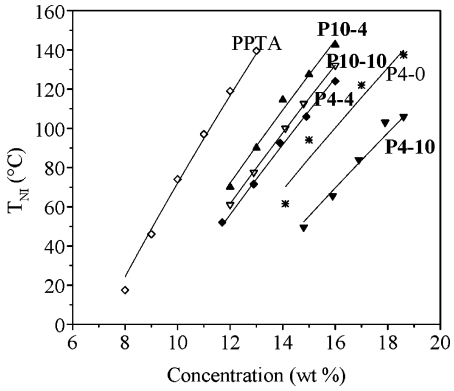

Figure 3. Clearing temperature T_{ni} at 50% phase separation as a function of polymer concentration in 100% H_2SO_4 of copolymer samples **P10-4**, **P10-10**, **P4-4**, and **P4-10,** PPTA (MW ~ 32 000), and a PPTA-oligomer with number of repeat units *n* of 4. Data points were fitted with the eq 7 with an α parameter of 2/3: $T_{ni} = Ac^{2/3}$, *A* values of PPTA of 73.7, **P10-4** of 65.8, **P10-10** of 63.8, **P4-4** of 62.8, **P4-0** of 58.7, and **P4-10** of 53.9 were found.

would be expected around 16 wt % since the copolymer contains about 50% PPTA. However, the phase transition already occurs at about 11 wt %, indicating that the polyamide coils are significantly stretched and therefore actually contribute to the stability of the LC phase.

b. Comparison of Phase Behavior with an Extended Maier−Saupe (EMS) Theory. Next we will compare our results to a modified Maier−Saupe mean-field theory developed by Picken.[11] The original Maier−Saupe (MS) theory[9,10] is developed for low molecular weight thermotropic liquid crystals and is based on a mean-field potential *U* that can be written as

$$U = -\epsilon\langle P_2\rangle P_2(\cos\beta) \tag{1}$$

and describes the influence of a nematic field on the orientation of one particle in that field. The strength of the potential is given by the parameter ϵ. $P_2(\cos\beta) = {}^1/_2(3\cos^2\beta - 1)$ is the second-order Legendre polynomial of cos β, and $\langle P_2\rangle$ is the average value, weighted by the orientational distribution function, of the Legendre polynomial $P_2(\cos\beta)$ and is usually called the order parameter. $\langle P_2\rangle$ is 0 in the case of an isotropic phase and would be 1 in the case of perfect molecular alignment.

Solving the self-consistency equation

$$\langle P_2\rangle = \frac{\int_{-1}^{1} \mathrm{d}(\cos\beta)\, P_2(\cos\beta) \exp\left(\frac{\epsilon}{kT}\langle P_2\rangle P_2(\cos\beta)\right)}{\int_{-1}^{1} \mathrm{d}(\cos\beta) \exp\left(\frac{\epsilon}{kT}\langle P_2\rangle P_2(\cos\beta)\right)} \tag{2}$$

as well as requiring minimization of the free energy with respect to $\langle P_2\rangle$ gives a phase transition at $kT/\epsilon \approx 0.22$ from the nematic (N) to the isotropic (I) phase. The critical value of the order parameter $\langle P_2\rangle$ at the phase transition is about 0.43. Picken[11] adapted the original Maier−Saupe theory for application to lyotropic polymer liquid crystals. This model takes, in contrast to the original MS theory, both the influence of the concentration of the polymer in a solvent and molecular flexibility of the polymer into account since LC polymers are not completely rigid. The molecular flexibility of a LC polymer is often described by the persistence length, which is a measure of the tendency of segments in a polymer chain to "remember" the orientation of adjoining segments in the chain.[14] The persistence length is a measure for the rigidity of a polymer in a specific solvent at ambient temperature and can be obtained from light-scattering experiments. In the modified Maier−Saupe theory the "contour projection length" $L(T)$ was introduced, which like the persistence length is a measure of the rigidity of a polymer but is a function of both temperature and molecular weight as given by

$$L(T) = L_p \frac{1 - \exp\left(-\frac{L_c T}{L_p T_p}\right)}{T/T_p} \tag{3}$$

where L_p is the persistence length at temperature T_p and L_c is the average contour length of a polymer chain. The limit of this equation for infinitely long polymer chains gives $L_c \cong L_p T_p/T$ and for a very short molecule (compared to the persistence length) $L(T) \cong L_c$, i.e., the length of a rod. Next it is assumed that the strength of the potential can be given by

$$\epsilon = \epsilon^* c^\gamma L^\delta(T) = \epsilon^* c^2 L^2(T) \tag{4}$$

where ϵ^* is a scaling constant and *c* the concentration. Our choice for the exponents γ and δ (both 2) is based on the

observation that dispersive van der Waals interactions scale as $1/r$,[6] where r is the distance between molecules. This dependence is proportional to $1/V^2$ or c^2, where V is the volume. The value for of the δ parameter is not easily estimated. Assuming that ϵ is proportional to L, i.e., $\delta = 1$, would seem reasonable from the perspective that increasing the length of a rod in a nematic environment would increase the orienting potential by the same amount. But on the other hand, one can argue that the Maier−Saupe potential is a generalized two-particle interaction leading to an L^2 dependence. Reasonable values for δ are thus somewhere between 1 and 2. When comparing the calculations with the experiments we, however, will use the value of the 2 since it has been shown by Picken[11] that for aramid systems dissolved in sulfuric acid this value for δ gives the best agreement with the experimental results. Substitution of eq 3 into eq 4 leads to

$$\epsilon = \epsilon^* c^2 L_p^2 \left(\frac{1 - \exp\left[-\frac{L_c T}{L_p T_p} \right]}{T/T_p} \right)^2 \tag{5}$$

At the nematic−isotropic transition temperature T_{ni} it was already shown that $kT_{ni}/\epsilon \approx 0.22$ holds; as a consequence, at T_{ni} eq 5 can be written as

$$\epsilon^* c_{ni}^2 L^2(T_{ni}) = kT_{ni}/0.22 \tag{6}$$

Rearrangement of this equation provides a prediction of the clearing temperature on the concentration that can be approximated quite well by

$$T_{ni} = A c_{ni}^{\alpha} \tag{7}$$

where A and α are constants. For the infinite chain limit, i.e., $L_c \gg L_p$ it can be derived that $\alpha = 2/3$. Clearing temperature vs concentration behavior of the polymer samples displayed in Figure 3 was fitted with eq 7 with a fixed parameter α of 2/3. From Figure 3 it is clear for all polymer samples that there is a remarkable good fit with eq 7.

c. Estimation of the Effective Persistence Length of the PPTA-*b*-PA 6,6 Block Copolymers with the Extended Maier−Saupe Theory. At a fixed value of T_{ni} the terms on the right-hand side of eq 6 are all constant and it can be simplified further to

$$c_{ni} L(T_{ni}) = \text{const} \tag{8}$$

This also means that the product $c_{ni}L$ at T_{ni} of PPTA is equal to $c_{ni}L$ at T_{ni} of the copolymer, or written slightly differently

$$\frac{c_{ni,PPTA}}{c_{ni,copolymer}} = \frac{L_{copolymer}(T_{ni})}{L_{PPTA}(T_{ni})} \tag{9}$$

If we can also neglect the influence of molecular weight on the flexibility, i.e., if the molecular weight of the copolymer is sufficiently high that its flexibility can be characterized by the persistence length, then eq 9 can be further simplified into

$$\frac{c_{ni,PPTA}}{c_{ni,copolymer}} = \frac{L_{p,copolymer}}{L_{p,PPTA}} \tag{10}$$

From light scattering experiments in dilute solution in H_2SO_4 it is found that the persistence length of PPTA at ambient temperature is 29 ± 5 nm.[15] From eq 10 therefore the persistence length of the block copolymer $L_{p,copolymer}$ can be estimated if we know the c_{ni} of PPTA and the copolymer at temperature T_{ni}, which can easily be determined from the phase diagrams. The results of the calculation of the persistence length for our copolymers are given in Table 2.

Table 2. Estimated Persistence Lengths of High MW PPTA and the Copolymers

polymer	critical concn for (I-LC) phase transition at T = 25 °C (wt %)	L_p according to phase behavior (via eq 10) (nm)	L_p according to series model (via eq 11) (nm)
PPTA ($M_w \approx 32\,000$)	8.1	29	29
P10-4	10.3	24.3	20.6
P10-10	10.3	23.7	15.0
P4-4	15.0	22.4	15.0
P4-10	13.8	18.1	9.4

An alternative way to calculate the persistence length of the copolymer is by taking the weighted average of the persistence lengths of the individual polymers. As a result, a series model is obtained

$$L_{p,copolymer} = \phi_{PPTA} L_{p,PPTA} + \phi_{PA6,6} L_{p,PA6,6} \tag{11}$$

where $L_{p,PA6,6}$ is the persistence length of PA 6,6, which is about 1.0 nm.[16,17] A series model is chosen because this should be considered as the upper bound of the copolymer persistence length in the absence of specific interactions of the LC phase on the flexible segment conformation. Values for the persistence lengths of our copolymer samples calculated from the series model are also shown in Table 2.

From this table it is clear that the persistence lengths of the copolymers obtained from the Maier−Saupe theory with phase transition data obtained from the phase diagram are significantly higher than predicted by the series model which indicates that the polyamide coils in the copolymer are significantly stretched by the mesophase.

Solid-State Properties. a. Effect of Copolymer Composition on Thermal Behavior Using DSC. DSC analysis of the block copolymer samples is shown in Figures 4 and 5. Figure 4 shows the DSC traces from the second heating scan of all copolymer samples. From this figure it is clear that crystallization of PA 6,6 is to a large extent hindered by the presence of PPTA. Only samples **P4-10** and **P10-10** show a melting peak for PA 6,6 but the melting points (T_m = 217 °C for **P4-10** and T_m = 208 °C for **P10-10**) are strongly reduced compared to the melting point of pure PA 6,6 ($T_m \approx 265$ °C). For copolymer samples with short polyamide chains (**P4-4** and **P10-4**) crystallization of the PA 6,6 is fully suppressed. Traditionally, melting point depression can be described by means of the Hoffmann−

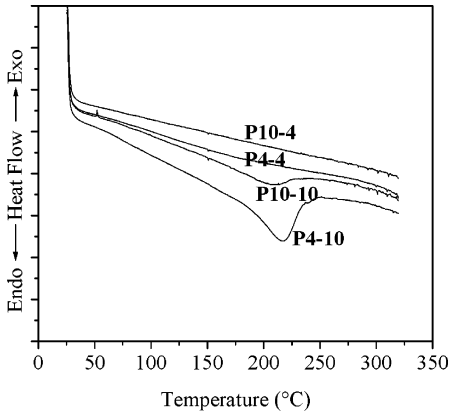

Figure 4. DSC plots of the copolymers.

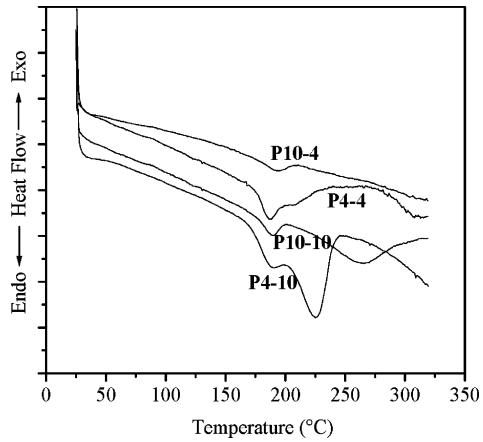

Figure 5. DSC plots of the annealed copolymers.

Weeks[18] equation. The melting point of a semicrystalline polymer according to this equation is given by

$$T_m = T_m^\circ\left(1 - \frac{2\gamma_e}{\Delta H_f l_c}\right) \tag{12}$$

where T_m is the observed (typically 265 °C) and T_m° the equilibrium melting point (T_m° = 300 °C for PA 6,6[19]), γ_e the surface free energy, ΔH_f the heat of fusion, and l_c the lamellar crystal thickness. If PA 6,6 crystallites melt in a matrix that only contains PA 6,6, the surface free energy between matrix and crystallites is (much) smaller than if PA 6,6 crystallites melt in a matrix that also contains PPTA. Therefore, with increasing PPTA content in the copolymer the PA 6,6 melting point should reduce if the lamellar crystal thickness remains constant. From Figure 4 it is clear that the melting point of **P4-10** is higher than for **P10-10** whereas the polyamide block length remains constant.

To investigate the melting of PA 6,6 by introducing PPTA in more detail, DSC analysis was performed on all copolymer samples after annealing overnight at a temperature of 160 °C. Figure 5 shows the curves of the first heating scan. It is clear that the annealing process induces crystallization since all copolymer samples show at least one melting peak. The overall degree of crystallinity increases with increasing the fraction of polyamide and with increasing the length of the polyamide blocks, as expected. The sequence of the degree of crystallinity is **P4-10** > **P10-10** > **P4-4** > **P10-4**.

Remarkably, all polymer samples show a melting peak around 190 °C, but for copolymer samples **P4-10**, **P10-10**, and **P4-4** also a second melting peak is observed at respectively 225, 267, and 310 °C. This shift to a higher melting point might be explained by a better-developed phase separation due to the annealing process, which induces higher orientation of the PA 6,6 coils. The improved orientation of the coils decreases the conformational entropy, and as a consequence the melting point increases since $T_m = \Delta H/\Delta S$.

It is expected that the glass transition temperature of the PA in the rod−coil copolymers considered here will progressively increase with increasing amount of PPTA because the mobility of the amorphous polyamide chains will be significantly constrained by the surrounding PPTA chains. However, with the DSC apparatus we have used no clear glass transition was observed in the DSC curves even for the sample with the highest the amount of PA (**P4-10**). DMA measurements will be performed in order to detect glass transitions of the PA 6,6 blocks. The results of the DMA measurements will be presented in a following paper.

b. Microstructure of PPTA-*b*-PA 6,6 Copolymers Using SAXS. SAXS measurements were performed on copolymer samples **P10-4**, **P4-4**, and **P4-10**. For each sample two diffraction patterns were recorded, one at a temperature far below the melting point of PA and one above the melting point of the PA blocks. The intensity of the small angle scattering depends on the composition ratio and the difference of the electron densities of the rigid and flexible component ($\rho_R - \rho_F$):

$$I(q) \sim \phi_R\phi_F(\rho_R - \rho_F)^2 \tag{13}$$

where ϕ_R and ϕ_F are the volume fraction of rigid and flexible segments, respectively.

The Lorentz correction was made on the scattering intensity according to

$$I(q)^* = 4\pi q^2 I(q) \tag{14}$$

where $I(q)$ is the observed scattering intensity and $I(q)^*$ is the corrected intensity. This correction compensates for the random orientations of periodic systems[20] and results in the peaks being sharpened and moved to slightly higher q values, compared to the uncorrected SAXS curves. SAXS profiles of our block copolymer samples are shown in Figure 6. For each block copolymer sample first a measurement was made above the melting point of the polyamide blocks. Next, the sample was cooled, and a second measurement was made at a temperature far below the melting point of the polyamide blocks.

The position of the scattering maxima, q_{max} can be used to estimate L_{obs}, the average observed long period of the structure given by

$$L_{obs} = \frac{2\pi}{q_{max}} \tag{15}$$

If we assume that the domains repeat one-dimensionally, we can calculate the long spacing as the sum of the domain lengths of a rigid block and a flexible block ($L_{cal} = L_R + L_F$). If, for the sake of simplicity, the effect of molecular weight distribution of both components is not taken into account, the rigid-segment domain length L_R for a perfect rigid rod is the product of the monomer length a and the degree of polymerization DP_R.

$$L_R = aDP_R \tag{16}$$

In the case of a perfect lamellar rearrangement in a rod−coil multiblock copolymer, the flexible coil segments will not be able to adopt a Gaussian conformation and as a consequence would be significantly stretched. A schematic illustration of such a lamellar phase is shown in Figure 7.

The length of the flexible domain can be calculated if the mass of the rigid and flexible domains is known. The mass of a rigid domain M_R can be written as

$$M_R = L_R A\rho_R \tag{17}$$

where A is the interfacial area between a rigid and flexible domain and ρ_R the density of the rods. The mass of a rigid domain can also be given by

$$M_R = Nm_R DP_R \tag{18}$$

where N is the number of rods and m_R the mass of the rod repeat unit. Similar equations can be written for a flexible coil domain:

$$M_F = L_F A\rho_F = Nm_F DP_F \tag{19}$$

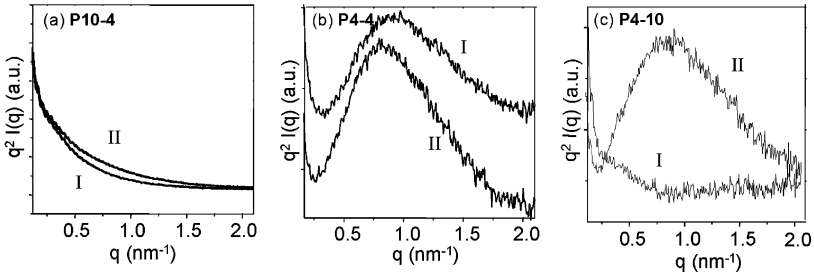

Figure 6. SAXS images of copolymer samples **P10-4** (a) measured at $T = 25$ °C (I) and $T = 220$ °C (II), **P4-4** (b) measured at $T = 25$ °C (I) and $T = 260$ °C (II), and **P4-10** (c) measured at $T = 50$ °C (I) and $T = 230$ °C (II).

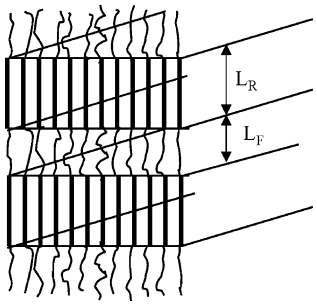

Figure 7. Schematic illustration of a lamellar structure of a multiblock rod−coil block copolymer.

where M_F is the mass of a flexible domain, ρ_F the density, m_F the mass of a repeat unit of the flexible coils, and DP_F the degree of polymerization of the coils. The number of coils in a domain is the same as the number of rods N. The length of the flexible domain L_F can be calculated by substitution of eqs 16, 17, and 18 into eq 19 and is given by

$$L_F = \frac{\rho_R}{\rho_F}\frac{m_F}{m_R} a DP_F \qquad (20)$$

The densities of amorphous PA 6,6 and PPTA are respectively 1.14 and 1.44 g/cm^3.

Figure 6 reveals that all copolymers show different patterns. Sample **P10-4** shows no peak in SAXS. This can possibly be explained by assuming that the small PA blocks are more or less randomly distributed in the rigid polymer and therefore do not phase separate into an ordered structure. Sample **P4-4** is the only sample that shows a peak in SAXS both above and below the melting point of PA. The observed peaks, however, are rather broad, and the spectrum shows no higher order peaks. This observation is typical for block copolymers obtained via a polycondensation method having a rather high polydispersity index. Sample **P4-10** only shows a peak in SAXS at high temperature. Since crystallization of the PA blocks in this polymer will increase its density, the density contrast between regions with rigid and flexible blocks will be reduced. The crystallization destroys the ordering and reduces density contrast, which leads to no scattering peaks at room temperature. After the melting of PA 6,6, the ordering is reconstructed, and a clear scattering peak appears in the small-angle X-ray scattering pattern. Since **P4-4** does not crystallize at room temperature as well as at high temperature, there is no destruction effect of the phase-separated layer structure from crystallization. The SAXS curve of sample **P4-4** measured above the melting point of PA 6,6 is sharper, indicating a more developed phase separation compared to the curve measured at ambient temperature. Because the phase separation is better developed, the polyamide coils are more stretched and the observed peak is shifted to a lower q value.

Table 3. SAXS Results

polymer	temp (°C)	L_{obs} (nm)	L_F (nm)	L_R (nm)	L_{cal} (nm)
P4-10	20		7.0	13.6	20.6
	220		7.0	13.6	20.6
P4-4	25	7.1	7.0	5.8	12.8
	230	7.7	7.0	5.8	12.8
P10-4	50		16.2	5.8	22.0
	230	7.7	16.2	5.8	22.0

Results for the observed long spacings L_{obs} for our copolymers samples are given in Table 3 and are much smaller than the calculated values L_{cal} of a lamellar phase.

An explanation for this large difference might be because a perfect lamellar arrangement in which the coils are significantly stretched is highly unfavorable in terms of entropy. This strong entropic penalty can be reduced if the sheetlike rod domains break up into smaller domains. In this case the flexible coils are less confined because they can occupy space lateral to the rigid-segment domains, and as a result the observed long period is significantly decreased.[13,21,22]

Assigning a structure simply by comparing the observed and the measured long order is for our copolymers not straightforward because the observed peaks in SAXS are rather broad because of the high polydispersity index.

Conclusions

Four rod−coil block copolymers differing in block length were synthesized which are composed of alternating flexible PA 6,6 and rigid PPTA blocks. Concentrated solutions of these copolymers in sulfuric acid are liquid crystalline if the aramid content in the copolymer is at least 50 mol %. The phase behavior of these solutions demonstrates that the liquid crystallinity involves induced orientation of the flexible polyamide coils because liquid crystallinity of the block copolymer is found to occur at a lower polymer concentration compared to a PPTA oligomer with the same block length. This means that the incorporation of aramid blocks in the copolymer induces stretching of the flexible coils, and this stretching will make the copolymer stiffer than expected initially. Complementary to the study on the LC behavior of the copolymer samples reported here, we intend to study the orientational order of the LC solutions by means of X-ray scattering. Results of this work will be presented in a following paper.

SAXS and DSC measurements were undertaken to study solid-state properties of the prepared block copolymer. DSC measurements revealed that crystallization of the PA blocks was to a large content suppressed by the presence of the aramid blocks. In addition, the melting point of the amide blocks is decreased strongly due to the presence of the aramid blocks. The SAXS curves obtained from polymer samples **P4-4** and **P4-10** showed a broad peak, indicating microphase separation that was not very well developed. This observation is also supported by the absence of higher order peaks. In addition,

the observed periodicity is significantly smaller than that expected for a perfect lamellar phase. Therefore, it is plausible to suppose a less well-developed broken lamellar or cylindrical phase where the long period is strongly reduced to diminish the unfavorable entropic penalty for chain stretching of the flexible coils.

We expect that this type of block copolymers will display interesting mechanical properties. We believe that films and fibers of this kind of polymer will combine a high modulus in the alignment direction due to the liquid crystallinity and also will display high-energy absorption because of the combination of the rigid segments providing stiffness and flexible segment providing elasticity. The study of the mechanical properties in relation to the structure of both copolymer fibers and films will be treated in a subsequent paper.

Acknowledgment. The research described here is part of the research program of FOM (Fundemental Onderzoek der Materie/Fundamental Research on Matter) in the Evolution of the Microstructure of Materials (EMM), project EMM14.

References and Notes

(1) De Ruijter, C.; Jager, W. F.; Groenewold, J.; Picken, S. J. *Macromolecules*, in press.
(2) Krigbaum, W. R.; Shufan, Z.; Preston, J.; Ciferri, A.; Conio, G. *J. Polym. Sci., Part B: Polym. Phys.* **1987**, *25*, 1043−1055.
(3) Cavalleri, P.; Ciferri, A.; Dell'Erba, C.; Novi, M.; Purevsuren, B. *Macromolecules* **1997**, *30*, 3513−3518.
(4) Cavalleri, P.; Ciferri, A.; Dell'Erba, C.; Gabellini, A.; Novi, M. *Macromol. Chem. Phys.* **1998**, *199*, 2087−2094.
(5) Matheson, R. R., Jr.; Flory, P. J. *Macromolecules* **1981**, *14*, 954−960.
(6) Vasilenko, S. V.; Khokhlov, A. R.; Shibaev, V. P. *Macromolecules* **1984**, *17*, 2270−2275.
(7) Yurasova, T. A.; Semenov, A. N. *Mol. Cryst. Liq. Cryst.* **1991**, *199*, 301.
(8) Wang, X. J.; Warner, M. *Liq. Cryst.* **1992**, *12*, 385−401.
(9) Maier, W.; Saupe, A. *Z. Naturforsch.* **1959**, *14A*, 882−889.
(10) Maier, W.; Saupe, A. *Z. Naturforsch.* **1960**, *15A*, 287−292.
(11) Picken, S. J. *Macromolecules* **1989**, *22*, 1766−1771.
(12) Flory, P. J. *Macromolecules* **1978**, *11*, 1138−1141.
(13) Lee, M.; Cho, B.-K.; Oh, N.-K.; Zin, W.-C. *Macromolecules* **2001**, *34*, 1987−1995.
(14) Xu, Z. D.; Hadjichristidis, N.; Fetters, L. J.; Mays, J. W. *Adv. Polym. Sci.* **1995**, *120*, 1−50.
(15) Ying, Q. C.; Chu, B. *Makromol. Chem., Rapid Commun.* **1984**, *5*, 785−791.
(16) Taylor, G. B. *J. Am. Chem. Soc.* **1947**, *69*, 638−644.
(17) Howard, G. J. *J. Polym. Sci.* **1959**, *37*, 310−313.
(18) Hoffman, J. D.; Weeks, J. J. *J. Res. Natl. Bur. Stand.* **1962**, *A66*, 13−28.
(19) Magill, J. H.; Girolamo, M.; Keller, A. *Polymer* **1981**, *22*, 43−55.
(20) Roe, R.-J. In *Methods of X-ray and Neutron Scattering in Polymer Science*; Oxford University Press: New York, 2000.
(21) Williams, D. R. M.; Fredrickson, G. H. *Macromolecules* **1992**, *25*, 3561−3568.
(22) Sakurai, S.; Okamoto, Y.; Sakaue, H.; Nakamura, T.; Banda, L.; Nomura, S. *J. Polym. Sci., Part B: Polym. Phys.* **2000**, *38*, 1716−1728.

MA052230+